Progress In Electromagnetics Research, PIER 9, 117–136, 1994

THE THEORY OF DYADIC GREEN'S FUNCTION AND THE RADIATION CHARACTERISTICS OF SOURCES IN STRATIFIED BI-ISOTROPIC MEDIA

W. Yin, P. Li, and W. Wang

1. Introduction

Recently, the interaction of electromagnetic waves with bianisotropic and bi-isotropic media have been examined by many authors, due to their wide applications in the fields of integrated optical devices as well as in the microwave and millimeter wave regimes. Bianisotropic materials are characterized by linear constitutive relations that couple the electric–and the magnetic–field vectors by four independent tensors, when these tensors reduce to scalar quantities, the bianisotropic media become bi-isotropic. Until now, certain properties of these complex media have been found and several interesting phenomena have been reported in the literature. For example, charged particles in bianisotropic media [1, 2], radiation and scattering in homogeneous general bi-isotropic regions [3], dispersion relation for bianisotropic material and its symmetry properties [4], reflection and transmission for planar structures of bianisotropic media [5], the interaction of electromagnetic waves with general bianisotropic slabs [6], vector transmission–line and circuit theory for bi-isotropic layered structures and a bi-isotropic layer as a polarization transformer [7, 8]. As a special case of the most general bi-isotropic medium, reciprocal chiral media are characterized by only three scalar parameters, and they have attracted much attention in the electromagnetics community recently [9–12].

We know, spectral DGF combining Fourier transform with matrix analysis methods can be used in a much more expedient way to investigate the radiation behavior of planar integrated structures [13]. However, the technique of eigenfunction expansion of DGF in conjunction with the numerical method is also very useful for the study of electromagnetic problems in multilayered media, waveguides, etc [14–16]. In this paper, the methods of eigenfunction expansion and scattering superposition are adopted for the constructing of DGF in unbounded and multilayered bi-isotropic media. Then, the influences of different parameters, especially, the cross electric and magnetic coefficients on the radiation patterns of dipole antenna in various bi-isotropic superstrate–substrate structures are examined carefully.

2. The Extended Eigenfunction Expansions of DGF in Unbounded Bi-isotropic Media

Bi-isotropic medium is electromagnetically characterized by the following set of constitutive relations for the time harmonic excitation ($e^{-i\omega t}$),

$$\overline{D} = \varepsilon\overline{E} + \xi_e\overline{H} \tag{1a}$$

$$\overline{B} = \mu\overline{H} + \xi_m\overline{E} \tag{1b}$$

where ε, μ, ξ_e, and ξ_m are the medium's permittivity, permeability, cross electric and magnetic coupling coefficients; the dimensions of ξ_e and ξ_m are inverse to that of speed. The bi-isotropic constitutive relations are obviously more general than that of reciprocal and nonreciprocal chiral media. For the case of nonreciprocal chiral media, ξ_e

and ξ_m may be given by

$$\xi_e = (\chi + i\kappa)\sqrt{\mu_0\varepsilon_0}, \xi_m = (\chi - i\kappa)\sqrt{\mu_0\varepsilon_0} \tag{2}$$

where the chirality parameter κ stands for the rate of polarization rotation of a propagating linearly polarized plane wave, relative to the rate of phase change of the wave in air: at a distance λ the rotation angle $\varphi = 2\pi\kappa$, and the Tellegen parameter χ causes polarization rotation for a plane wave normally incident from air, in reflection from a bi-isotropic interface.

Using (1) together with Maxwell equations, the electric field in a bi-isotropic medium should satisfy

$$\nabla \times \nabla \times \overline{E} - i\omega(\xi_m - \xi_e)\nabla \times \overline{E} - \omega^2(\mu\varepsilon - \xi_e\xi_m)\overline{E} = i\omega\mu\overline{J}_e \tag{3}$$

and

$$\overline{E}(\overline{R}) = i\omega\mu \int_v \overline{\overline{G}}(\overline{R}|\overline{R}') \cdot \overline{J}(\overline{R}')dv' \tag{4}$$

in which the DGF of $\overline{\overline{G}}(\overline{R}|\overline{R}')$ is determined by

$$\nabla \times \nabla \times \overline{\overline{G}}(\overline{R}|\overline{R}') - i\omega(\xi_m - \xi_e)\nabla \times \overline{\overline{G}}(\overline{R}|\overline{R}') - \omega^2(\mu\varepsilon - \xi_e\xi_m)\overline{\overline{G}}(\overline{R}|\overline{R}')$$
$$= \overline{I}\delta(\overline{R} - \overline{R}') \tag{5}$$

Eq. (5) can be solved in terms of normalized cylindrical vector wave functions $\{\overline{L}_{\substack{e\\o}n\lambda}(h), \overline{V}_{\substack{e\\o}n\lambda}(h), \overline{W}_{\substack{e\\o}n\lambda}(h)\}$ in a circular cylinder coordinate system (r, φ, z) , which have been defined in [12] and [17]. The orthogonal properties of these functions are stated as follows:

$$\int_v \overline{L}_{\substack{e\\o}n\lambda}(h) \cdot \overline{V}_{\substack{e\\o}n'\lambda'}(-h')dv = 0, \quad \int_v \overline{L}_{\substack{e\\o}n\lambda}(h) \cdot \overline{W}_{\substack{e\\o}n'\lambda'}(-h')dv = 0 \tag{6a, b}$$

$$\int_v \overline{L}_{\substack{e\\o}n\lambda}(h) \cdot \overline{L}_{\substack{e\\o}n'\lambda'}(-h')dv = 2\pi^2 k^2 \frac{(1 + \delta_{no})}{\lambda} \delta(\lambda - \lambda')\delta(h - h')\delta_{nn'} \tag{6c}$$

$$\int_v \overline{V}_{\substack{e\\o}n\lambda}(h)\cdot\overline{V}_{\substack{e\\o}n'\lambda'}(-h')dv = \int_v \overline{W}_{\substack{e\\o}n\lambda}(h)\cdot\overline{W}_{\substack{e\\o}n'\lambda'}(-h')dv$$

$$=2\pi^2\lambda(1+\delta_{no})\delta(\lambda-\lambda')\delta(h-h')\delta_{nn'}$$

$$(6d, e)$$

where the domain of integration encloses the entire space, h is the longitudinal wave number $h^2 = k^2 - \lambda^2, \delta(\bullet)$ is Dirac delta function, and δ_{no} and $\delta_{nn'}$ are the Kronecker delta, given by

$$\delta_{no} = \begin{cases} 1 & n = 0 \\ 0 & n \neq 0 \end{cases},$$

$$\delta_{nn'} = \begin{cases} 1 & n = n' \\ 0 & n \neq n' \end{cases} \tag{7}$$

Using the Ohm-Rayleigh method, the right-hand side of (5) is expressed by

$$\overline{I}\delta(\overline{R}-\overline{R}')$$

$$= \int_0^{+\infty} d\lambda \int_{-\infty}^{+\infty} dh \sum_{n=0}^{\infty} \frac{2-\delta_{no}}{4\pi^2\lambda}$$

$$\cdot\left[\frac{\lambda^2}{k^2}\overline{L}'_{\substack{e\\o}n\lambda}(-h)\overline{L}_{\substack{e\\o}n\lambda}(h) + \overline{V}'_{\substack{e\\o}n\lambda}(-h)\overline{V}_{\substack{e\\o}n\lambda}(h) + \overline{W}'_{\substack{e\\o}n\lambda}(-h)\overline{W}_{\substack{e\\o}n\lambda}(h)\right] \tag{8}$$

and

$$\overline{\overline{G}}(\overline{R}|\overline{R}') = \int_0^{+\infty} d\lambda \int_{-\infty}^{+\infty} dh \sum_{n=0}^{\infty} \frac{2-\delta_{no}}{4\pi^2\lambda}$$

$$\cdot\Bigg[A(\lambda)\overline{V}'_{\substack{e\\o}n\lambda}(-h)\overline{V}_{\substack{e\\o}n\lambda}(h) + B(\lambda)\overline{W}'_{\substack{e\\o}n\lambda}(-h)\overline{W}_{\substack{e\\o}n\lambda}(h)$$

$$+ C(\lambda)\frac{\lambda^2}{k^2}\overline{L}'_{\substack{e\\o}n\lambda}(-h)\overline{L}_{\substack{e\\o}n\lambda}(h)\Bigg] \tag{9}$$

and substituting (9) and (8) into (5), we find

$$\left\{ \begin{array}{c} A(\lambda) \\ B(\lambda) \end{array} \right\} = \frac{1}{(k \mp k_+)(k \pm k_-)}, \tag{10a}$$

$$C(\lambda) = -\frac{1}{\omega^2 \mu\varepsilon (1 - \frac{\xi_e \xi_m}{\mu\varepsilon})} \tag{10b}$$

where $k_\pm = \pm \frac{i\omega(\xi_m - \xi_e)}{2} + \omega\sqrt{\varepsilon\mu - \frac{(\xi_m + \xi_e)^2}{4}}$ are the wave numbers corresponding to the two circularly polarized modes propagating in unbounded bi-isotropic medium; the RCP mode propagates with wave number k_+, and the LCP modes with k_-. In (9), the integration with respect to h can be calculated using the method of contour integration, it is given by

$$\begin{aligned}
&\overline{\overline{G}}(\overline{R}|\overline{R}') \\
&= -\frac{\overline{e}_z \overline{e}_z \delta(\overline{R} - \overline{R}')}{k_0^2(1 - \frac{\xi_e \xi_m}{\mu\varepsilon})} + \frac{i}{2\pi(k_+ + k_-)} \int_0^{+\infty} d\lambda \sum_{n=0}^{\infty} \frac{2 - \delta_{no}}{\lambda} \\
&\quad \left\{ \frac{k_+}{h_+} \left[\begin{array}{l} \overline{V}_{\substack{e\\o}n\lambda}(h_+)\overline{V}'_{\substack{e\\o}n\lambda}(-h_+) \\ \overline{V}_{\substack{e\\o}n\lambda}(-h_+)\overline{V}'_{\substack{e\\o}n\lambda}(h_+) \end{array} \right] \right. \\
&\quad \left. + \frac{k_-}{h_-} \left[\begin{array}{l} \overline{W}_{\substack{e\\o}n\lambda}(h_-)\overline{W}'_{\substack{e\\o}n\lambda}(-h_-) \\ \overline{W}_{\substack{e\\o}n\lambda}(-h_-)\overline{W}'_{\substack{e\\o}n\lambda}(h_-) \end{array} \right] \right\} \begin{array}{l} z \geq z' \\ z \leq z' \end{array}
\end{aligned} \tag{11}$$

Also, we can perform the integration with respect to λ in (9), given by

$$\begin{aligned}
&\overline{\overline{G}}(\overline{R}|\overline{R}') \\
&= -\frac{\overline{e}_z \overline{e}_z \delta(\overline{R} - \overline{R}')}{k_0^2(1 - \frac{\xi_e \xi_m}{\mu\varepsilon})} + \frac{i}{4\pi(k_+ + k_-)} \int_{-\infty}^{+\infty} dh \sum_{n=0}^{\infty} (2 - \delta_{n0})
\end{aligned}$$

$$
\left\{\frac{k_+}{\eta_+^2}\begin{bmatrix}\overline{V}^{(1)}_{\substack{e\\o}n\eta_+}(h)\overline{V}'_{\substack{e\\o}n\eta_+}(-h)\\ \overline{V}_{\substack{e\\o}n\eta_+}(-h)\overline{V}^{(1)'}_{\substack{e\\o}n\eta_+}(h)\end{bmatrix}\right.
$$

$$
\left.+\frac{k_-}{\eta_-^2}\begin{bmatrix}\overline{W}^{(1)}_{\substack{e\\o}n\eta_-}(h)\overline{W}'_{\substack{e\\o}n\eta_-}(-h)\\ \overline{W}_{\substack{e\\o}n\eta_-}(-h)\overline{W}^{(1)'}_{\substack{e\\o}n\eta_-}(h)\end{bmatrix}\right\}\begin{matrix}r\geq r'\\ r\leq r'\end{matrix} \tag{12}
$$

where $\eta_\pm = \sqrt{k_\pm^2 - h^2}$. (11) and (12) are the extended eigenfunction expansions of DGF in unbounded bi-isotropic media, which are similar to the DGF of reciprocal chiral media [12]. However, the singular term of (11) and (12) in the source region is different from the chiral case [9].

Following the similar procedure used above, the eigenfunction expansion of DGF in the unbounded bi-isotropic medium can be also obtained using normalized elliptical cylinder vector wave functions (appendix). Unfortunately, the technique of eigenfunction expansion is not valid for the bianisotropic case, and the spectral-domain DGF may be derived using Fourier transform method.

3. The Formulations of DGF for the Stratified Bi-isotropic Media

The problem of multilayered reciprocal cylindrical chiral media, excited by an arbitrarily electric or magnetic source, has been treated by us in [12] and lead to compact closed-form expressions of DGF. The extension of the analysis to multilayered bi-isotropic media will be carried out here.

The geometrical configuration of n-layer bi-isotropic medium is shown in Fig. 1. For any layer (j), the constitutive relations are given as (1):

$$
\overline{D}_j = \varepsilon_j\overline{E}_j + \xi_{ej}\overline{H}_j, \tag{13a}
$$

$$
\overline{B}_j = \mu_j\overline{H}_j + \xi_{mj}\overline{E}_j \tag{13b}
$$

$$
j = 1, 2, \ldots, n
$$

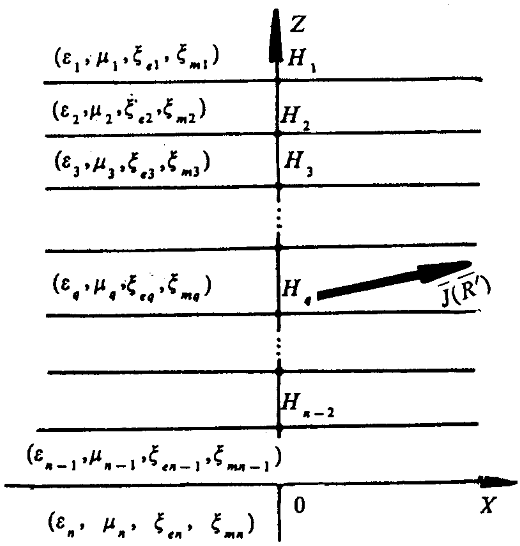

Figure 1. The multilayered bi-isotropic media.

and the wave numbers corresponding to RCP and LCP modes in layer (j) are

$$k_{j\pm} = \pm \frac{i\omega(\xi_{mj} - \xi_{ej})}{2} + \omega\sqrt{\varepsilon_j \mu_j - \frac{(\xi_{ej} + \xi_{mj})^2}{4}} \tag{14}$$

Supposing the impressed source $\overline{J}(\overline{R}')$ is electric and is located inside the layer (q) of bi-isotropic media, $\overline{\overline{G}}_q(\overline{R}|\overline{R}')$ can be expressed as a superposition of the unbounded $\overline{\overline{G}}_{qo}(\overline{R}|\overline{R}')$ that is due to the primary-source excitation and the scattered DGF, thus

$$\overline{\overline{G}}_q(\overline{R}|\overline{R}') = \overline{\overline{G}}_{qo}(\overline{R}|\overline{R}') + \overline{\overline{G}}_{qs}(\overline{R}|\overline{R}') \tag{15}$$

where

$$\overline{\overline{G}}_{q0}(\overline{R}|\overline{R}')$$

$$= -\frac{\overline{e}_z\overline{e}_z\delta(\overline{R}-\overline{R}')}{k_{q0}^2(1-\frac{\xi_{eq}\xi_{mq}}{\mu_q\varepsilon_q})} + \frac{i}{2\pi(k_{q+}+k_{q-})}\int_0^{+\infty} d\lambda \sum_{n=0}^{\infty}\frac{2-\delta_{n0}}{\lambda}$$

$$\cdot\left\{\frac{k_{q+}}{h_{q+}}\begin{bmatrix}\overline{V}_{\substack{e\\o}n\lambda}(h_{q+})\overline{V}'_{\substack{e\\o}n\lambda}(-h_{q+})\\ \overline{V}_{\substack{e\\o}n\lambda}(-h_{q+})\overline{V}'_{\substack{e\\o}n\lambda}(h_{q+})\end{bmatrix}\right.$$

$$\left.+\frac{k_{q-}}{h_{q-}}\begin{bmatrix}\overline{W}_{\substack{e\\o}n\lambda}(h_{q-})\overline{W}'_{\substack{e\\o}n\lambda}(-h_{q-})\\ \overline{W}_{\substack{e\\o}n\lambda}(-h_{q-})\overline{W}'_{\substack{e\\o}n\lambda}(h_{q-})\end{bmatrix}\right\},\ \begin{matrix}z'\le z\\ z\le z'\end{matrix} \tag{16}$$

and

$$\overline{\overline{G}}_{qs}(\overline{R}|\overline{R}') = \frac{i}{2\pi(k_{q+}+k_{q-})}\int_0^{+\infty} d\lambda \sum_{n=0}^{\infty}\frac{2-\delta_{n0}}{\lambda}$$

$$\cdot\left\{\frac{k_{q+}}{h_{q+}}\left\{[A_{n1}^q\overline{V}_{\substack{e\\o}n\lambda}(-h_{q+}) + A_{n2}^q\overline{W}_{\substack{e\\o}n\lambda}(-h_{q-})]\overline{V}'_{\substack{e\\o}n\lambda}(-h_{q+})\right.\right.$$

$$\left.+[A_{n3}^q\overline{V}_{\substack{e\\o}n\lambda}(-h_{q+}) + A_{n4}^q\overline{W}_{\substack{e\\o}n\lambda}(-h_{q-})]\overline{V}'_{\substack{e\\o}n\lambda}(h_{q+})\right\}$$

$$+\frac{k_{q-}}{h_{q-}}\left\{[A_{n5}^q\overline{V}_{\substack{e\\o}n\lambda}(-h_{q+}) + A_{n6}^q\overline{W}_{\substack{e\\o}n\lambda}(-h_{q-})]\overline{W}'_{\substack{e\\o}n\lambda}(-h_{q-})\right.$$

$$\left.+[A_{n7}^q\overline{V}_{\substack{e\\o}n\lambda}(-h_{q+}) + A_{n8}^q\overline{W}_{\substack{e\\o}n\lambda}(-h_{q-})]\overline{W}'_{\substack{e\\o}n\lambda}(h_{q-})\right\}$$

$$+\frac{k_{q+}}{h_{q+}}\left\{[B_{n1}^q\overline{V}_{\substack{e\\o}n\lambda}(h_{q+}) + B_{n2}^q\overline{W}_{\substack{e\\o}n\lambda}(h_{q-})]\overline{V}'_{\substack{e\\o}n\lambda}(-h_{q+})\right.$$

$$\left.+[B_{n3}^q\overline{V}_{\substack{e\\o}n\lambda}(h_q+) + B_{n4}^q\overline{W}_{\substack{e\\o}n\lambda}(h_{q-})]\overline{V}'_{\substack{e\\o}n\lambda}(h_{q+})\right\}$$

$$+\frac{k_{q-}}{h_{q-}}\left\{[B_{n5}^q\overline{V}_{\substack{e\\o}n\lambda}(h_{q+}) + B_{n6}^q\overline{W}_{\substack{e\\o}n\lambda}(h_{q-})]\overline{W}'_{\substack{e\\o}n\lambda}(-h_{q-})\right.$$

$$+\left[B^q_{n7}\overline{V}_{\substack{e\\o}n\lambda}(h_{q+})+B^q_{n8}\overline{W}_{\substack{e\\o}n\lambda}(h_{q+})\right]\overline{W}'_{\substack{e\\o}n\lambda}(h_{q-})\Big\}\Big\}$$

$$\tag{17}$$

where $k^2_{q0}=\omega^2\mu_q\varepsilon_q, h_{q\pm}=\sqrt{k^2_{q\pm}-\lambda^2}$. The DGF in layer (1), layer (j) $(j\neq q)$ and layer (n) must have the following forms, given by

$$\begin{aligned}
\overline{\overline{G}}_1(\overline{R}|\overline{R}')=&\frac{i}{2\pi(k_{q+}+k_{q-})}\int_0^{+\infty}d\lambda\sum_{n=0}^{\infty}\frac{2-\delta_{n0}}{\lambda}\\
&\cdot\Big\{\frac{k_{q+}}{h_{q+}}\Big\{\left[A^1_{n1}\overline{V}_{\substack{e\\o}n\lambda}(h_{1+})+A^1_{n2}\overline{W}_{\substack{e\\o}n\lambda}(h_{1-})\right]\overline{V}'_{\substack{e\\o}n\lambda}(-h_{q+})\\
&+\left[A^1_{n3}\overline{V}_{\substack{e\\o}n\lambda}(h_{1+})+A^1_{n4}\overline{W}_{\substack{e\\o}n\lambda}(h_{1-})\right]\overline{V}'_{\substack{e\\o}n\lambda}(h_{q+})\Big\}\\
&+\frac{k_{q-}}{h_{q-}}\Big\{\left[A^1_{n5}\overline{V}_{\substack{e\\o}n\lambda}(h_{1+})+A^1_{n6}\overline{W}_{\substack{e\\o}n\lambda}(h_{1-})\right]\\
&\overline{W}'_{\substack{e\\o}n\lambda}(-h_{q-})+\left[A^1_{n7}\overline{V}_{\substack{e\\o}n\lambda}(h_{1+})+A^1_{n8}\overline{W}_{\substack{e\\o}n\lambda}(h_{1-})\right]\overline{W}'_{\substack{e\\o}n\lambda}(h_{q-})\Big\}\Big\}
\end{aligned}\tag{18}$$

$$\begin{aligned}
\overline{\overline{G}}_j(\overline{R}|\overline{R}')=&\frac{i}{2\pi(k_{q+}+k_{q-})}\int_0^{+\infty}d\lambda\sum_{n=0}^{\infty}\frac{2-\delta_{n0}}{\lambda}\\
&\cdot\Big\{\frac{k_{q+}}{h_{q+}}\Big\{\left[A^j_{n1}\overline{V}_{\substack{e\\o}n\lambda}(-h_{j+})+A^j_{n2}\overline{W}_{\substack{e\\o}n\lambda}(-h_{j-})\right]\overline{V}'_{\substack{e\\o}n\lambda}(-h_{q+})\\
&+\left[A^j_{n3}\overline{V}_{\substack{e\\o}n\lambda}(-h_{j+})+A^j_{n4}\overline{W}_{\substack{e\\o}n\lambda}(-h_{j-})\right]\overline{V}'_{\substack{e\\o}n\lambda}(h_{q+})\Big\}\\
&+\frac{k_{q-}}{h_{q-}}\Big\{\left[A^j_{n5}\overline{V}_{\substack{e\\o}n\lambda}(-h_{j+})+A^j_{n6}\overline{W}_{\substack{e\\o}n\lambda}(-h_{j-})\right]\overline{W}'_{\substack{e\\o}n\lambda}(-h_{q-})\\
&+\left[A^j_{n7}\overline{V}_{\substack{e\\o}n\lambda}(-h_{j+})+A^j_{n8}\overline{W}_{\substack{e\\o}n\lambda}(-h_{j-})\right]\overline{W}'_{\substack{e\\o}n\lambda}(h_{q-})\Big\}\\
&+\frac{k_{q+}}{h_{q+}}\Big\{\left[B^j_{n1}\overline{V}_{\substack{e\\o}n\lambda}(h_{j+})+B^j_{n2}\overline{W}_{\substack{e\\o}n\lambda}(h_{j-})\right]\overline{V}'_{\substack{e\\o}n\lambda}(-h_{q+})\\
&+\left[B^j_{n3}\overline{V}_{\substack{e\\o}n\lambda}(h_{j+})+B^j_{n4}\overline{W}_{\substack{e\\o}n\lambda}(h_{j-})\right]\overline{V}'_{\substack{e\\o}n\lambda}(h_{q+})\Big\}
\end{aligned}$$

$$
\begin{aligned}
&+\frac{k_{q-}}{h_{q-}}\Big\{[B^j_{n5}\overline{V}_{\genfrac{}{}{0pt}{}{e}{o}n\lambda}(h_{j+})+B^j_{n6}\overline{W}_{\genfrac{}{}{0pt}{}{e}{o}n\lambda}(h_{j-})]\overline{W}'_{\genfrac{}{}{0pt}{}{e}{o}n\lambda}(-h_{q-})\\
&+[B^j_{n7}\overline{V}_{\genfrac{}{}{0pt}{}{e}{o}n\lambda}(h_{j+})+B^j_{n8}\overline{W}_{\genfrac{}{}{0pt}{}{e}{o}n\lambda}(h_{j-})]\overline{W}'_{\genfrac{}{}{0pt}{}{e}{o}n\lambda}(h_{q-})\Big\}\Big\},\\
&\qquad j=2,3,\ldots,q-1,q+1.\ldots,n-1
\end{aligned}
\tag{19}
$$

$$
\begin{aligned}
&\overline{\overline{G}}_n(\overline{R}|\overline{R}')=\frac{i}{2\pi(k_{q+}+k_{q-})}\int_0^{+\infty}d\lambda\sum_{n=0}^{\infty}\frac{2-\delta_{n0}}{\lambda}\\
&\cdot\Big\{\frac{k_{q+}}{h_{q+}}\Big\{[A^n_{n1}\overline{V}_{\genfrac{}{}{0pt}{}{e}{o}n\lambda}(-h_{n+})+A^n_{n2}\overline{W}_{\genfrac{}{}{0pt}{}{e}{o}n\lambda}(-h_{n-})]\overline{V}'_{\genfrac{}{}{0pt}{}{e}{o}n\lambda}(-h_{q+})\\
&+[A^n_{n3}\overline{V}_{\genfrac{}{}{0pt}{}{e}{o}n\lambda}(-h_{n+})+A^n_{n4}\overline{W}_{\genfrac{}{}{0pt}{}{e}{o}n\lambda}(-h_{n-})]\overline{V}'_{\genfrac{}{}{0pt}{}{e}{o}n\lambda}(h_{q+})\Big\}\\
&+\frac{k_{q-}}{h_{q-}}\Big\{[A^n_{n5}\overline{V}_{\genfrac{}{}{0pt}{}{e}{o}n\lambda}(-h_{n+})+A^n_{n6}\overline{W}_{\genfrac{}{}{0pt}{}{e}{o}n\lambda}(-h_{n-})]\overline{W}'_{\genfrac{}{}{0pt}{}{e}{o}n\lambda}(-h_{q-})\\
&+[A^n_{n7}\overline{V}_{\genfrac{}{}{0pt}{}{e}{o}n\lambda}(-h_{n+})+A^n_{n8}\overline{W}_{\genfrac{}{}{0pt}{}{e}{o}n\lambda}(-h_{n-})]\overline{W}'_{\genfrac{}{}{0pt}{}{e}{o}n\lambda}(h_{q-})\Big\}\Big\}
\end{aligned}
\tag{20}
$$

In (17)–(20), $A^q_{n1}-A^q_{n8}$, $B^q_{n1}-B^q_{n8}$, $A^1_{n1}-A^1_{n8}$, $A^j_{n1}-A^j_{n8}$, $B^j_{n1}-B^j_{n8}$, $A^n_{n1}-A^n_{n8}$, are the unknown coefficients by the boundary conditions at $z=H_1,H_2,\ldots,H_{n-2},0$. Since the transverse electric and magnetic fields across the interfaces are continuous, with the help of (13) and Maxwell's equations, we easily find

$$
\overline{e}_z\times\overline{\overline{G}}_q(\overline{R}|\overline{R}')=\overline{e}_z\times\overline{\overline{G}}_{q+1}(\overline{R}|\overline{R}'),\qquad z=H_q
\tag{21}
$$

$$
\begin{aligned}
&\overline{e}_z\times[\frac{1}{\mu_q}\nabla\times\overline{\overline{G}}_q(\overline{R}|\overline{R}')]-\overline{e}_z\times\frac{i\omega\xi_{mq}}{\mu_q}\overline{\overline{G}}_q(\overline{R}|\overline{R}')\\
&=\overline{e}_z\times[\frac{1}{\mu_{q+1}}\nabla\times\overline{\overline{G}}_{q+1}(\overline{R}|\overline{R}')]-\overline{e}_z\times\frac{i\omega\xi_{mq+1}}{\mu_{q+1}}\overline{\overline{G}}_{q+1}(\overline{R}|\overline{R}'),\\
&z=H_q
\end{aligned}
\tag{22}
$$

On the other hand, when the impressed source in layer (q) is a magnetic current $\overline{J}_m(\overline{R}')$, $\overline{\overline{G}}_q(\overline{R}|\overline{R}')$, and $\overline{\overline{G}}_{q+1}(\overline{R}|\overline{R}')$ should satisfy

$$\begin{aligned} \overline{e}_z \times \overline{\overline{G}}_q(\overline{R}|\overline{R}') =& \overline{e}_z \times \overline{\overline{G}}_{q+1}(\overline{R}|\overline{R}'), \\ z =& H_q \end{aligned} \tag{23}$$

$$\begin{aligned} &\overline{e}_z \times \left[\frac{1}{\varepsilon_q}\nabla \times \overline{\overline{G}}_q(\overline{R}|\overline{R}')\right] + \overline{e}_z \times \frac{i\omega\xi_{eq}}{\varepsilon_q}\overline{\overline{G}}_q(\overline{R}|\overline{R}') \\ &= \overline{e}_z \times \left[\frac{1}{\varepsilon_{q+1}}\nabla \times \overline{\overline{G}}_{q+1}(\overline{R}|\overline{R}')\right] + \overline{e}_z \times \frac{i\omega\xi_{eq+1}}{\varepsilon_{q+1}}\overline{\overline{G}}_{q+1}(\overline{R}|\overline{R}'), \\ &z = H_q \end{aligned} \tag{24}$$

Substituting (15)–(20) into (21)–(22), yields four sets of $4(n-1)$ linear equations. When the $(n-1)-$ layer bi-isotropic media are bounded by a perfectly conducting plane at $z = 0$ in Fig. 1, we have

$$\overline{e}_z \times \overline{\overline{G}}_{n-1}(\overline{R}|\overline{R}')|_{z=0} = 0 \tag{25}$$

and the unknown coefficients in (17)–(20) are determined by four sets of $2(2n-1)$ linear equations.

In numerically solving the four sets of $4(n-1)$ linear equations, the computer time required becomes cumbersome as the number of layers increases. An efficient method for calculating the unknown coefficients for an arbitrary number of layers can be utilized based on transmission matrix technique. With respect to the structure of Fig. 1, if the electromagnetic parameters of inhomogeneous bi-isotropic layer are described by $\varepsilon = \varepsilon(z), \mu = \mu(z), \xi_e = \xi_e(z), \xi_m = \xi_m(z), (0 < z < H_1)$, an approximate DGF can also be found in this case by artificially dividing the whole region $(0 < z < H_1)$ into $n-2$ sublayers. For sufficiently small $\triangle H_q(q = 1, 2, \ldots, n-1)$ one may assume a constant value for each of the scalar quantities $(\varepsilon_q, \mu_q, \xi_{eq}, \xi_{mq})$ inside each sublayer, thus the field distributions excited by an arbitrary source embedded in the inhomogeneous bi-isotropic slab can be obtained in terms of the expressions of DGF derived above.

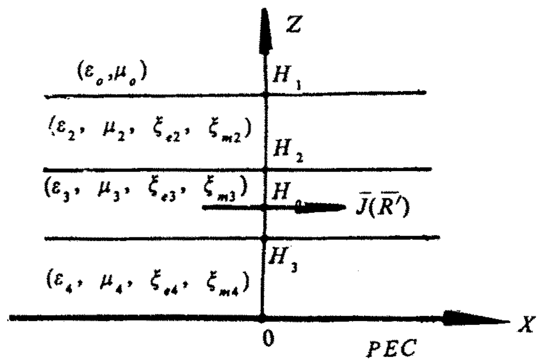

Figure 2. Dipole antenna in a bi-isotropic four-layer geometry.

4. The Radiation Patterns of a Dipole Antenna in Stratified Bi-isotropic Media

In microstrip antenna technology, it is often necessary to examine the radiation characteristics of dipoles printed in a superstrate–substrate structure. The geometry of interest is shown in Fig. 2, and the electric current density of dipole antenna is given by

$$\overline{J}(\overline{R}') = \overline{e}_x I_0 \delta(x)\delta(y)\delta(z - H_0), \qquad H_3 \le H_0 \le H_2 \tag{26}$$

Then, the electric field in layer (1) is determined by

$$\overline{E}_1(\overline{R}) = i\omega\mu_3 \int_{v'} \overline{\overline{G}}_1(\overline{R}|\overline{R}') \cdot \overline{J}(\overline{R}')dv' \tag{27}$$

where $\overline{\overline{G}}_1(\overline{R}|\overline{R}')$ has been shown by (18)(q=3). Noticing that

$$\int_0^{+\infty} J_n(\lambda r) f(\lambda) d\lambda = \int_{-\infty}^{+\infty} H_n^{(1)}(\lambda r) f(\lambda) d\lambda \tag{28}$$

where $J_n(\lambda r)$ and $H_n^{(1)}(\lambda r)$ are the first kind of Bessel and Hankel function with order n, respectively. In the far zone $(\lambda r >> 1)$,

$$\begin{bmatrix} \overline{V}^{(1)}_{\substack{e\\o}n\lambda}(h_{1+}) \\ \overline{W}^{(1)}_{\substack{e\\o}n\lambda}(h_{1-}) \end{bmatrix} \approx (-i)^{n+\frac{1}{2}} \frac{\lambda}{\sqrt{\pi\lambda r}} e^{i(\lambda r + h_{1\pm} z)} \frac{\cos}{\sin}(n\varphi) \cdot \left(-i\overline{e}_\varphi \pm \frac{\lambda \overline{e}_z - h_{1\pm}\overline{e}_r}{k_{1\pm}} \right) \tag{29}$$

and by taking advantage of the stationary phase asymptotic integration, we obtain

$$\begin{aligned} \overline{E}_1(\overline{R}) = &-\frac{\omega\mu_3 I_0}{4\pi R(k_{3+}+k_{3-})} \cos\theta \frac{\cos}{\sin}(\varphi) \Bigg\{ [A^1_{11} k_{1+} e^{ik_{1+}R}(\overline{e}_\theta + i\overline{e}_\varphi) \\ &- A^1_{12} k_{1-} e^{ik_{1-}R}(\overline{e}_\theta - i\overline{e}_\varphi)] e^{-ik_{3+}H_0} \left(\frac{k_{3+}}{h_{3+}} - i \right) \\ &+ [A^1_{13} k_{1+} e^{ik_{1+}R}(\overline{e}_\theta + i\overline{e}_\varphi) - A^1_{14} k_{1-} e^{ik_{1-}R}(\overline{e}_\theta - i\overline{e}_\varphi)] \\ &\qquad e^{ik_{3+}H_0} \left(\frac{k_{3+}}{h_{3+}} + i \right) \\ &+ [A^1_{15} k_{1+} e^{ik_{1+}R}(\overline{e}_\theta + i\overline{e}_\varphi) - A^1_{16} k_{1-} e^{ik_{1-}R}(\overline{e}_\theta - i\overline{e}_\varphi)] \\ &\qquad e^{-ik_{3-}H_0} \left(\frac{k_{3-}}{h_{3-}} + i \right) \\ &+ [A^1_{17} k_{1+} e^{ik_{1+}R}(\overline{e}_\theta + i\overline{e}_\varphi) - A^1_{18} k_{1-} e^{ik_{1-}R}(\overline{e}_\theta - i\overline{e}_\varphi)] \\ &\qquad e^{ik_{3-}H_0} \left(\frac{k_{3-}}{h_{3-}} + i \right) \Bigg\} \end{aligned} \tag{30}$$

where $h_{3\pm} = \sqrt{k^2_{3\pm} - k^2_{1\pm}\sin^2\theta}$, and $A^1_{11} - A^1_{18}$ are determined by four sets of 14 linear equations. In (30), the sums $(\overline{e}_\theta + i\overline{e}_\varphi)$ and $(\overline{e}_\theta - i\overline{e}_\varphi)$ indicate RCP and LCP modes; it is worth noting that the radiated field emitted by dipole antenna is in general elliptically polarized.

The far-field behavior of dipole antennas in various composite bi-isotropic superstrate-substrate configurations are presented in Figs. 3, 4, and 5. Since the properties of a bi-isotropic medium have never been completely characterized either at optical or microwave frequencies, we had to assume the material properties used in the calculations. The values used for the constitutive parameter are close to what are

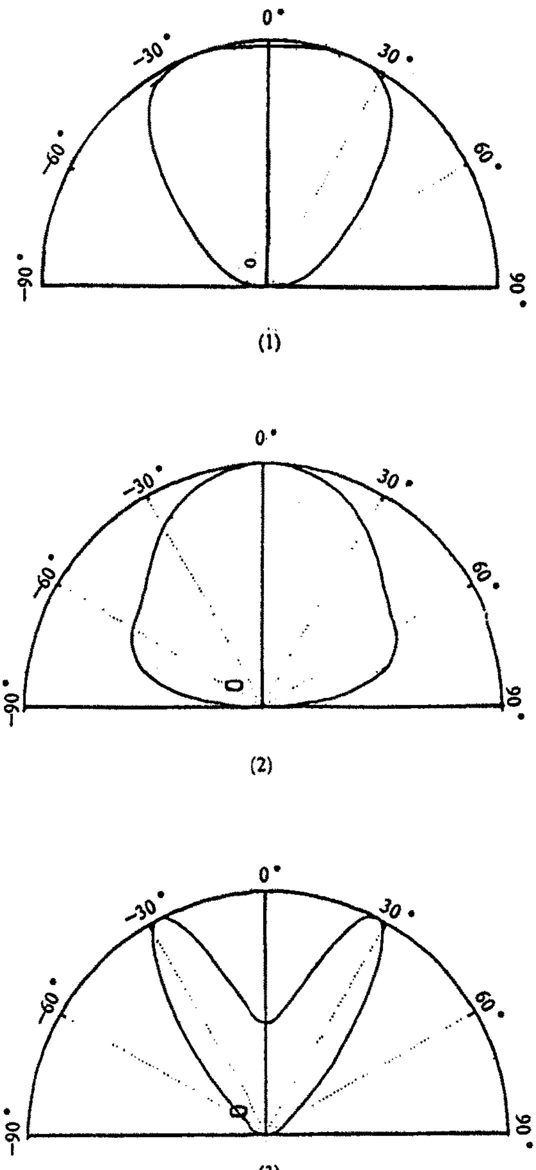

Figure 3. **The radiation pattern of dipole antenna in a bi-isotropic three-layer geometry.** $H_1 = 0.03\text{m}, H_2 = 0.02\text{m}, H_3 = 0.01\text{m}, H_0/\lambda = 0.5, \phi = 0, 90°, \mu_2 = \mu_3 = \mu_4 = \mu_0, \epsilon_3 = 2\epsilon_2, \epsilon_4 = 2\epsilon_3$, **(1)** $\xi_{e2} = \xi_{m2}^* = i3.0 \times 10^{-11}, \xi_{e3} = \xi_{m3}^* = 10\xi_{e2}, \xi_{e4} = \xi_{m4}^* = 10\xi_{e3}$ **(reciprocal chiral). (2)** $\xi_{e2} = \xi_{m2}^* = (2.5 + i3.0) \times 10^{-11}, \xi_{e3} = \xi_{m3}^* = (5.0 + i6.0) \times 10^{-10}, \xi_{e4} = \xi_{m4}^* = (8.0 + i10) \times 10^{-9}$ **(nonreciprocal chiral). (3)** $\xi_{e2} = 2\xi_{m2}^* = (2.5 + i3.0) \times 10^{-11}, \xi_{e3} = 2\xi_{m3}^* = (5.0 + i6.0) \times 10^{-10}, \xi_{e4} = 2\xi_{m4}^* = (8.0 + i10) \times 10^{-9}$.
*** standards for the complex conjugate.**

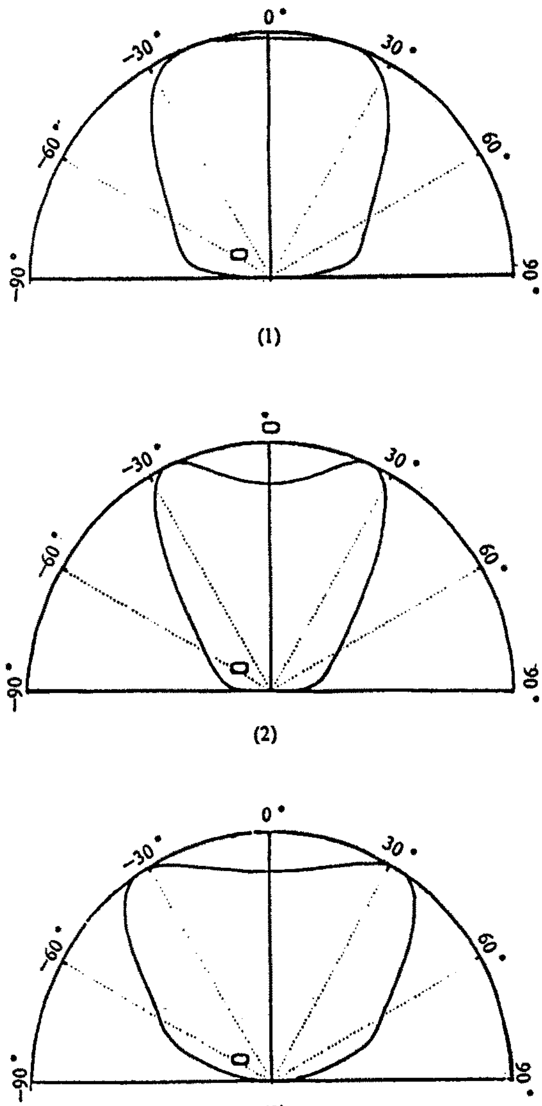

Figure 4. The radiation pattern of dipole antenna in a bi-isotropic two-layer geometry. $H_1 = 0.03\text{m}, H_3 = 0.01\text{m}, H_0/\lambda = 0.3333, \phi = 0, 90° \epsilon_2 = 2\epsilon_3 = 2.5\epsilon_0$ **(1)** $\epsilon_4 = 5.0\epsilon_0, \xi_{e2} = \xi_{e3} = 2\xi^*_{m2} = 2\xi^*_{m3} = i3.0 \times 10^{-11}, \xi_{e4} = 2\xi^*_{m4} = i3.0 \times 1010^{-10}$. **(2)** $\epsilon_4 = 5.0\epsilon_0, \xi_{e2} = \xi_{e3} = 0.1\xi^*_{m2} = 0.1\xi^*_{m3} = i3.0 \times 10^{-11}, \xi_{e4} = 0.1\xi^*_{m4} = i3.0 \times 1010^{-10}$. **(3)** $\epsilon_4 = \epsilon_0, \xi_{e2} = \xi^*_{m2} = i3.0 \times 10^{-11}, \xi_{e4} = \xi^*_{m4} = 0$.

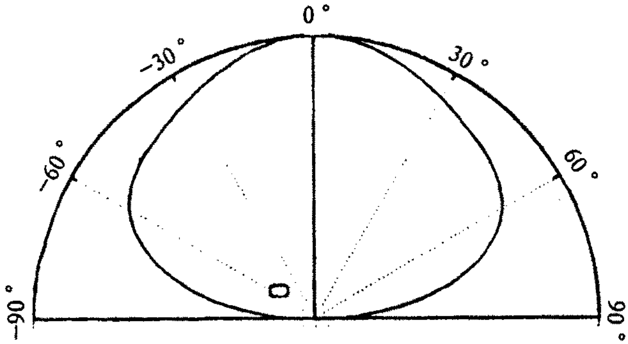

Figure 5. The radiation pattern of dipole antenna in a grounded bi-isotropic slab. $\phi = 0, 90°, \mu_2 = \mu_0, H_1 = 0.02\text{m}, H_0/\lambda = 0.3333, \epsilon_2 = 2.5\epsilon_0, \xi_{e2} = \xi^*_{m2} = i3.0 \times 10^{-11}$ **(reciprocal chiral slab).**

reported in the literature [7, 8] and in all the examples, it is assumed that the top layer (1) is air and the operating frequency is taken to be $f = 10\,\text{GHz}$.

The numerical results have shown, in the case of an electric x-oriented point source, that the radiation patterns present a symmetry with respect to vertical axis $(\theta = 0°)$, and suitable pattern resharping are made by choosing the cross electric and magnetic coupling coefficients of bi-isotropic media. In order to demonstrate the effects of ξ_e and ξ_m, reciprocal $(\xi_e = \xi^*_m = i\kappa)$ and nonreciprocal chiral media $(\xi_e = \xi^*_m = \chi + i\kappa)$ are also taken into consideration. Fig. 5 shows the special case of a grounded reciprocal chiral slab, which has been studied by Engheta and Vegni [11], however, the source is embedded inside the chiral slab and is not placed on the surface.

5. Conclusion

The general formulation of DGF for the electric or magnetic sources embedded inside multilayered bi-isotropic media has been given and the radiation characteristics of dipole antennas in bi-isotropic superstrate-substrate structure have been investigated in detail. An important point to note is that the radiation behavior of the dipole antenna is a function of several different factors: superstrate and substrate thickness, permittivity, permeability, cross electric and magnetic couple coefficients, and operating frequency. The different appearance of the radiation patterns shown above depends on the combination of all of these factors.

Appendix

The vector wave functions $\{\overline{L}_{\substack{e\\o}m\lambda}(h), \overline{M}_{\substack{e\\o}m\lambda}(h), \overline{N}_{\substack{e\\o}m\lambda}(h)\}$ are orthogonal and normalized to each other in an elliptical cylinder coordinate system. Also, we introduce normalized elliptical cylinder vector wave functions:

$$\begin{bmatrix} \overline{V}_{\substack{e\\o}m\lambda}(h) \\ \overline{W}_{\substack{e\\o}m\lambda}(h) \end{bmatrix} = \frac{1}{\sqrt{2}}\left[\overline{M}_{\substack{e\\o}m\lambda}(h) \pm \overline{N}_{\substack{e\\o}m\lambda}(h)\right] \tag{A1}$$

Thus, the right-hand side of (5) is expressed by

$$\overline{I}\delta(\overline{R}-\overline{R}') = \int_0^{+\infty} d\lambda \int_{-\infty}^{+\infty} dh \sum_m \Big\{\overline{A}_{\substack{e\\o}m\lambda}(h)\overline{V}_{\substack{e\\o}m\lambda}(h) + \overline{B}_{\substack{e\\o}m\lambda}(h)\overline{W}_{\substack{e\\o}m\lambda}(h) + \overline{C}_{\substack{e\\o}m\lambda}(h)\overline{L}_{\substack{e\\o}m\lambda}(h)\Big\} \tag{A2}$$

and

$$\begin{bmatrix} \overline{A}_{\substack{e\\o}m\lambda}(h) \\ \overline{B}_{\substack{e\\o}m\lambda}(h) \end{bmatrix} = \frac{1}{\pi^2\lambda I_{\substack{e\\o}m\lambda}} \begin{bmatrix} \overline{V}'_{\substack{e\\o}m\lambda}(-h) \\ \overline{W}'_{\substack{e\\o}m\lambda}(-h) \end{bmatrix} \tag{A3a, b}$$

$$\overline{C}_{\substack{e\\o}m\lambda}(h) = \frac{1}{\pi^2\lambda I_{\substack{e\\o}m\lambda}} \overline{L}'_{\substack{e\\o}m\lambda}(-h) \tag{A3c}$$

where $I_{\substack{e\\o}m\lambda}$ is the normalized factor which may be calculated using series expansion method [17], and

$$\overline{\overline{G}}(\overline{R}|\overline{R}') = \int_0^{+\infty} d\lambda \int_{-\infty}^{+\infty} dh \sum_{n=0}^{\infty} \frac{1}{\pi^2 \lambda I_{{}^e_o m\lambda}}$$

$$\left[A(\lambda)\overline{V}'_{{}^e_o m\lambda}(-h)\overline{V}_{{}^e_o m\lambda}(h) + B(\lambda)\overline{W}'_{{}^e_o m\lambda}(-h)\overline{W}_{{}^e_o m\lambda}(h)\right] \quad (A4)$$

$$+\left[C(\lambda)\frac{\lambda^2}{k^2}\overline{L}'_{{}^e_o m\lambda}(-h)\overline{L}_{{}^e_o m\lambda}(h)\right]$$

The integrations with respect to λ and h are calculated, respectively, given as:

$$\overline{\overline{G}}(\overline{R}|\overline{R}') = -\frac{\overline{e}_u\overline{e}_u\delta(\overline{R}-\overline{R}')}{k_0^2(1-\frac{\xi_e\xi_m}{\mu\varepsilon})} + \frac{i}{\pi}\int_{-\infty}^{+\infty} dh \sum_m \frac{1}{(k_+ + k_-)}$$

$$\left\{\frac{k_+}{\eta_+^2 \overline{I}_{{}^e_o m\eta_+}}\begin{bmatrix}\overline{V}^{(1)}_{{}^e_o m\eta_+}(h)\overline{V}'_{{}^e_o m\eta_+}(-h)\\ \overline{V}_{{}^e_o m\eta_+}(-h)\overline{V}^{(1)'}_{{}^e_o m\eta_+}(h)\end{bmatrix}\right.$$

$$\left.+\frac{k_-}{\eta_-^2 I_{{}^e_o m\eta_-}}\begin{bmatrix}\overline{W}^{(1)}_{{}^e_o m\eta_-}(h)\overline{W}'_{{}^e_o m\eta_-}(-h)\\ \overline{W}_{{}^e_o m\eta_-}(-h)\overline{W}^{(1)'}_{{}^e_o m\eta_-}(h)\end{bmatrix}\right\} \quad \begin{matrix} u \geq u' \\ u \leq u' \end{matrix} \quad (A5)$$

where $\eta_\pm = \sqrt{k_\pm^2 - h^2}, \overline{e}_u$ is the unit vector, and

$$\overline{\overline{G}}(\overline{R}|\overline{R}')$$

$$= \frac{-\overline{e}_z\overline{e}_z\delta(\overline{R}-\overline{R}')}{k_0^2(1-\frac{\xi_e\xi_m}{\mu\varepsilon})} + \frac{2i}{\pi}\int_0^{+\infty} d\lambda \sum_m \frac{1}{\lambda(k_+ + k_-)I_{{}^e_o m\lambda}}$$

$$\left\{\frac{k_+}{h_+}\begin{bmatrix}\overline{V}_{{}^e_o m\lambda}(h_+)\overline{V}'_{{}^e_o m\lambda}(-h_+)\\ \overline{V}_{{}^e_o m\lambda}(-h_+)\overline{V}'_{{}^e_o m\lambda}(h_+)\end{bmatrix}\right.$$

$$\left.+\frac{k_-}{h_-}\begin{bmatrix}\overline{W}_{{}^e_o m\lambda}(h_-)\overline{W}'_{{}^e_o m\lambda}(-h_-)\\ \overline{W}_{{}^e_o m\lambda}(-h_-)\overline{W}^{(1)'}_{{}^e_o m\lambda}(h_-)\end{bmatrix}\right\} \begin{matrix} z \geq z' \\ z \leq z' \end{matrix} \quad (A6)$$

This is the eigenfunction expansions of DGF in an elliptical cylinder coordinate system for the unbounded bi-isotropic medium.

Acknowledgments

This work was supported, in part, by the China National Natural Science and Ministry of Aerospace Industry Foundations.

References

1. Kong, J. A., "Charged particles in bianisotropic media," *Radio Science*, Vol. 6, 1015–1019, 1971.
2. Kong, J. A., "Theorems of bianisotropic media," *IEEE Proc.*, Vol. 60, 1036–1046, 1972.
3. Monzon, J. C., "Radiation and scattering in homogeneous general bi-isotropic regions," *IEEE Trans. Antennas Propagat.*, Vol. 38, 227–235, 1990.
4. Graglia, R. D., P. L. E. Uslenghi, and R. E. Zich, "Dispersion relation for bi-isotropic materials and its symmetry properties," *IEEE Trans. Antennas Propagat.*, Vol. 39, 83–89, 1991.
5. Graglia, R. D., P. L. E. Uslenghi, and R. E. Zich, "Reflection and transmission for planar structures of bianisotropic media," *Electromagnetics*, Vol. 11, 193–208, 1991.
6. Tsalamengas, J. L., "Interaction of electromagnetic waves with general bianisotropic structures," *IEEE Trans. Antennas and Propatgat.*, Vol. 40, No. 10, 1870–1878, 1992.
7. Lindell, I. V., S. A. Tretyakov, and M. I. Oksanen, "Vector transmission-line and circuit theory for bi-isotropic layered structures," *J. Electromagnetic Waves and Applications*, Vol. 7, No. 1, 147–173, 1993.
8. Tretyakov, S. A., M. I. Oksanen, "A bi-isotropic layer as a polarization transformer," *J. Electromagnetic Waves and Applications*, Vol. 6, No. 10, 1393–1411, 1992.
9. Ali, S. M., T. M. Habashy, and J. A. Kong, "Spectral-domain dyadic Green's function in layered chiral media," *J. Opt. Soc. Am. A*, Vol. 9, No. 3, 413–422, 1992.
10. He, S., "A time-harmonic Green's function technique and wave propagation in a stratified nonreciprocal chiral slab with multiple discontinuities," *J. Math. Phys.*, Vol. 33, No. 22, 1–8, 1992.

11. Toscano, A., and L. Vegni, "Spectral dyadic Green's function formulation for planar integrated structures with a grounded chiral slab," *J. Electromagnetic Waves and Applications,* Vol. 6, No. 5/6, 751–759, 1992.
12. Yin, W., and W. Wang, "Dyadic Green's function of cylindrical multilayered chiral media and its applications," *J. Electromagnetic Waves and Applications,* Vol. 7, No. 7, 1005–1027, 1993.
13. Vegni, L., R. Cichetti, and P. Capace, "Spectral dyadic Green's function formulation for planar integrated structures," *IEEE Trans. Antennas Propagat.,* Vol. 36, No. 8, 1057–1065, 1988.
14. Cavalcanto, G. P. S., D. A. Rogers, and A. J. Giarola, "Analysis of electromagnetic wave propagation in multilayered media using dyadic Green's function," *Radio Science,* Vol. 17, 503–508, 1982.
15. Fonseca, S., and A. Giarola, "Analysis of microstrip wraparound antennas using dyadic Green's functions," *IEEE Trans. Antennas Propagat.,* Vol. 31, No. 3, 248–253, 1983.
16. Silva, F. C., S. B. A. Fonseca, A. J. M. Soares, and A. J. Giarola, "Analysis of microstrip antennas on circular cylindrical substrates with a dielectric overlay," *IEEE Trans. Antennas Propagat.*, Vol. 39, No. 9, 1398–1403, 1991.
17. Tai, C. T., *Dyadic Green's Functions in Electromagnetic Theory,* Intert Educational Publishers, Scranton, PA, 1971.